Isı Bilimi ve Tekniği Dergisi, 37, 1, 1-12, 2017
J. of Thermal Science and Technology

ISSN 1300-3615

NATURAL CONVECTION OF WATER NEAR 4°C INSIDE PARTIALLY HEATED AND COOLED VERTICAL WALLS

Mehmet Akif EZAN* **and Mustafa KALFA****
Dokuz Eylül University, Faculty of Engineering, Mechanical Engineering Department, 35397 Buca, Izmir
*mehmet.ezan@deu.edu.tr, **mustafa_kalfa@windowslive.com

(Geliş Tarihi: 09.11.2015, Kabul Tarihi: 18.07.2016)

Abstract: In this study, transient heat transfer process inside a two-dimensional cavity has been numerically investigated. The numerical model has been created with control volume approach by using C++ programming language. In order to determine the accuracy of the numerical code, comparisons are made with the results of the numerical analysis and experimental velocity measurements from the literature. After that, the time-dependent variations of local and average Nusselt numbers have been revealed for various aspect ratios and different thermal boundary conditions of the cavity. The interaction of temperature and velocity distributions by different boundary conditions has been examined. In cold storage applications, water temperature decreases below the density inversion temperature and the natural convection of water becomes more complicated. Nevertheless, the majority of the models that are developed to simulate the cold storage units in the literature reduce the heat transfer mechanism into conduction mode to simplify the complexity of the coupled governing equations, so that take advantage of decreasing the computational time. Neglecting the complex convection currents may lead erroneous predictions. In this regard, the results of the current work will guide the researchers and the design engineers working on the cold storage applications with water as a storage medium.
Keywords: Transient natural convection, Density inversion, Partial heating/cooling, Aspect ratio

DÜŞEY DUVARLARI KISMİ ISITILAN VE SOĞUTULAN DUVARLAR İÇERİSİNDEKİ SUYUN 4°C CİVARINDAKİ DOĞAL TAŞINIMI

Özet: Bu çalışmada, iki boyutlu kavite içerisindeki zamana bağlı ısı transferi prosesi sayısal olarak incelenmiştir. Sayısal model kontrol hacimleri yaklaşımı kullanılarak C++ programlama dilinde oluşturulmuştur. Sayısal kodun doğruluğunu belirlemek için, literatürden alınan sayısal analiz sonuçları ve deneysel hız ölçümleri ile karşılaştırmalar yapılmıştır. Bundan sonra, çeşitli kavite görünüm oranları ve farklı ısıl sınır koşulları için zamana bağlı yerel ve ortalama Nusselt sayısı değişimleri ortaya koyulmuştur. Farklı sınır koşulları ile sıcaklık ve hız dağılımları arasındaki etkileşim incelenmiştir. Soğu depolama uygulamalarında su sıcaklığı yoğunluk dönüşüm sıcaklığının altına düşmekte ve suyun doğal taşınımı kompleks hale gelmektedir. Bununla beraber, literatürde soğu depolama ünitelerinin simülasyonu için geliştirilen modellerin büyük çoğunluğunda birleşik yönetici denklemlerin karmaşıklığını basitleştirmek adına ısı transferi mekanizması iletime indirgenmekte ve böylece çözüm süresinde önemli avantajlar elde edilebilmektir. Karmaşık taşınım akımlarının ihmal edilmesi hatalı tahminlere sebep olabilmektedir. Bu bağlamda, bu çalışmada elde edilecek sonuçlar, depolama ortamı olarak su kullanılan soğu depolama uygulamalarında çalışan araştırmacılara ve tasarım mühendislerine yol gösterici olacaktır.
Anahtar Kelimeler: Zamana bağlı doğal taşınım, Yoğunluk dönüşüm, Kısmi ısıtma/soğutma, Görünüm oranı

LIST OF SYMBOLS

A	Area [m^2]
c	Specific heat [$Jkg^{-1}K^{-1}$]
g	Gravitational acceleration [ms^{-2}]
H	Height of cavity [m]
k	Thermal conductivity [WmK^{-1}]
Nu	Nusselt number [-]
p	Pressure [Pa]
R	Density inversion parameter [-]
t	Time [s]
T	Temperature [K]
u, v	Velocity components [ms^{-1} / mm s^{-1}]
W	width of the cavity [m]
x, y	coordinates [m]
X	dimensionless horizontal coordinate [x/H]
Y	dimensionless vertical coordinate [y/H]

Greek Letters

ϕ	variable
ρ	density [kgm^{-3}]
μ	dynamic viscosity [$kgm^{-1}s^{-1}$]
θ	dimensionless temperature $(T-T_C)/(T_H-T_C)$
ξ	height of the active wall [m]

Subscripts

C	cold
H	hot
m	maximum density
ref	reference

INTRODUCTION

Natural (or *free*) convection is a buoyancy−driven heat transfer mechanism that occurs in fluids and governed by the temperature difference. It is widely encountered in thermal systems such as heating/cooling of buildings, drying of foods, thermal control of electronic devices, and thermal energy storage applications with or without phase change *(solid/liquid*). The temperature variations inside the fluid cause the density differences so that natural fluid motion occurs. Boussinesq approximation can be validly used to investigate the natural convection of the fluids that have linear density variations with respect to the temperature, such as air (Bergman *et al.*, 2011). On the other hand, the density variations of some liquids (i.e. water, gallium, and tellurium) are not defined linearly by temperature. After a certain temperature, the density variations become reversely proportional to increasing temperature. As an instance, the density of water increases with the temperature range of 0°C to 4°C. After 4°C, its density decreases with increasing temperature. Hence, 4°C is known as "*density inversion*" point in the literature (Seki *et al.* 1978; Inaba and Fukuda, 1984; Lin and Nansteel, 1987).

In Figure 1, three different cavities are illustrated to discuss the effect of density variations of water on natural convection. Here, the temperature of the right-hand side wall is kept as T_H, and the left one is also held as T_C. Under the steady−state condition, the flow structure inside the cavity is related to *density inversion* parameter (R).

$$R = \frac{T_m - T_c}{T_H - T_c} \tag{1}$$

where, T_m represents the temperature at a maximum density (for water $T_m = 4$°C). For $R < 0$ ($T_H > T_C > T_m$), the density of the fluid in the cavity increases from hot wall to cold wall. Therefore, a counter-clockwise single circulation cell is obtained inside the cavity (Figure 1a). For $R > 0$ ($T_m > T_H > T_C$), density increases from cold wall to hot wall, so that, a clockwise single circulation cell is obtained inside the cavity (Figure 1b). On the other hand, for $0 < R < 1$ ($T_H > T_m > T_C$), density increases from cold wall to hot wall, and it reaches the maximum value at T_m, beyond that point the density decreases. Thus, the flow structure inside the cavity is divided into two regions on T_m. While the clockwise rotated circulation cell is occurred on the left-hand side of the point T_m, the counter-clockwise cell is observed at the other part of the cavity (Figure 1c).

In the literature, the studies that have been conducted on the natural convection of water can be divided into two parts; *(i) steady state* and *(ii) time dependent*. Seki et al. (1978) investigated steady−state natural convection both numerically and experimentally in rectangular vessels that have various temperature differences and aspect ratios ($H/W = 1$ and 5). They have stated that unlike the common fluids that have linear density−temperature relationships, for the case of water, the average Nusselt number has a peculiar function of temperature difference between the side walls. Inaba and Fukudo (1984) analyzed the flow and temperature distribution of water inside an inclined cavity for different angles. Lin and Nansteel (1987) developed a numerical model of natural convection inside the square cavity for different Rayleigh numbers ($Ra = 10^3 - 10^6$) and density inversion parameters (R = 0.4, 1/2, 0.55, 2/3, 3/4 and 1). Hossain and Rees (2005) observed the steady−state natural convection inside a cavity for different aspect ratios driven by uniform heat generation. Braga and Viskanta (1992) and McDonough and Faghri (1994) investigated the transient heat transfer inside a cavity that was filled with water both numerically and experimentally. In the experimental measurements of the above mentioned works, helium−neon laser and pH−indicator methods were used to visualize the flow structures, respectively. The velocity distributions were presented based on various temperature differences inside the cavity. Wei and Koster (1994) studied transient natural convection inside cavities with different aspect ratios and temperature differences.

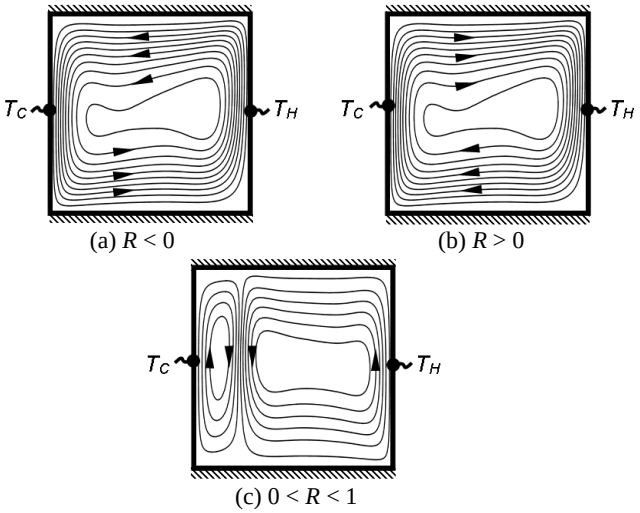

(a) $R < 0$ (b) $R > 0$

(c) $0 < R < 1$

Figure 1. Effect of density inversion parameter on natural convection

Banaszek *et al.* (1999) developed a semi−closed finite element method to investigate phase change problems including both convection and conduction effects of heat transfer. Transient heat transfer of water inside a square cavity was observed by using PIV (Particle – Image − Velocimetry) method to validate the accuracy of the numerical model. In experiments, one side of the cavity was kept at 10°C, and the other end was held at −10°C (or 0°C) to observe natural convection with (or *without*) phase change. Moraga and Vega (2004) generated two and three-dimensional models of the natural convection problem that has been already studied by Banaszek *et al.* (1999). They discussed the differences between those two models. Öğüt (2010) applied the polynomial differential quadrature (PDQ) method to resolve the natural convection of water based nano-fluids inside an inclined square cavity. Isotherms, streamlines and the dimensionless Nusselt number variations on the vertical walls were represented by varying the Rayleigh number, inclination angle, the fraction of nano-particle within the water. Öztuna and Kahveci (2013) developed a numerical code to solve the steady state natural convection within a partially divided square cavity. The code was based on the stream function/vorticity approach in which the thermos-physical

properties of water based nano-fluids were assumed to be independent of temperature. Rahimi *et al.* (2012) compared the local Nusselt number variations for the steady-state natural convection of pure water and nano-fluids within a square cavity. It is stated that increasing the volume fraction of the nano-particles within the base fluid, water, the local Nusselt number enhances. They also compared the usage of Boussinesq (*linear*) and non-Boussinesq (*non-linear*) approaches to simulate the temperature dependent density variations. It is interesting to note that the difference between the linear and non-linear density approaches is nearly 60%, regarding the average Nusselt number on the cold wall.

The reviewed studies so far were considered that the hot or cold walls were uniformly heated or cooled. However, in some particular conditions partitioned thermal boundary conditions may be subjected on the active walls. Such special cases may arise due to the shading, poor insulation or consciously located heating/cooling equipment, such as electronic components. Turkoglu and Yücel (1994) developed in−house CFD code to determine the influence of heater/cooler positions on the steady−state natural convection of air within a square enclosure. They varied the heated and cooled partitions on the side walls from bottom to top walls. It is stated that when the hot plate was located slightly above the bottom wall and the cooler was placed slightly below the top wall; the highest average Nusselt number was obtained. Nardini and Paroncini (2012) experimentally and numerically observed the effects of size and position of the heating and cooling elements in the vertical side walls on the natural convection of air. Tekkalmaz (2015), on the other hand, investigated the steady-state heat transfer within an air filled square enclosure for partially heated side wall. A combined numerical model was developed in a commercial CFD solver, ANSYS-FLUENT, with considering the natural convection and radiative heat transfer. Parametric analyses have been carried out by varying Rayleigh number ($10^5 \leq Ra \leq 10^7$) and surface emissivity ($0 \leq \varepsilon \leq 1$). Consequently, Nusselt correlations were proposed regarding the non-dimensional parameters.

Kandaswamy *et al.* (2007), Nithyadevi *et al.* (2007a) and Nithyadevi *et al.* (2007b) investigated transient natural convection of water in a cavity with partially active vertical walls. They have developed a numerical code with considering that, except density, the fluid properties are constant. Time−wise variations of average Nusselt numbers and velocity/temperature distributions were obtained for various aspect ratios of the cavity. Nithyadevi *et al.* (2007b) stated that the transient natural convection of water in a rectangular cavity with differentially heated side walls is mostly encountered in engineering and geophysical applications. Jmai *et al.* (2013) analyzed a total of six different heated wall configurations for a square cavity that was filled with nano-fluid. Steady state isotherms and stream functions were represented for locating the heated walls as Top–Top (TT), Top–Middle (TM), Top–Down (TD), Middle–Middle (MM), Middle–Down (MD), and Down–Down (DD). Rashidi et al. (2014) considered Al_2O_3 filled the square cavity with bottom wall subjected to a non–uniform heat flux. Top and left wall were assumed to be adiabatic, and the right wall was isothermal. Nine different heterogeneous heating scenarios have been analyzed. They also investigated the influences of Rayleigh number, nanoparticle volume fraction and aspect ratio of the cavity on the isotherms, streamlines and the Nusselt number under steady−state condition. In a recent work, Mahapatra et al. (2015) emphasized that there are many studies related to the square or rectangular cavities with different aspect ratios or partial heating/cooling boundary conditions in literature. However, they also stressed that the most of the studies in the literature are focused on representation of the heat transfer and flow pattern regarding Nusselt number and stream-function, rather than dealing with the temperature uniformity or thermal mixing.

Different research groups have analyzed the partial heating/cooling scenarios for the case of the air filled cavity. Nevertheless, there is a limited work in the literature in which the transient natural convection of water is investigated. In cold energy storage applications for near−zero temperatures, one of the best storage media is water (Heier *et al.* 2015). Either sensible or latent heat thermal storage systems, the temperature of the storage medium is mostly close to the density inversion temperature of water, especially for air conditioning applications (Li *et al.* 2012). The mathematical models of sensible and latent heat storage units should include the natural convection phenomena to design the thermal energy storage system properly. Since the computational cost of such coupled physics is quite expensive, recently some researchers suggest interpreting the influence of natural convection as an artificial effective (or *enhanced*) thermal conductivity. Ismail *et al.* (2005) and Ezan *et al.* (2014) proved that the effective thermal conductivity definition provides a better accuracy and lower computational times to simulate phase change problems inside spherical capsules. Investigating the transient nature of buoyancy driven heat transfer of water near the density maxima inside Cartesian coordinates, under various design and working conditions, can help the researchers in the field to simulate the coupled problems more accurately.

In this study, it is intended to develop a numerical code to simulate transient natural convection of water near its density maxima. Unlike the previous studies, in the current work the thermos-physical properties of the water are defined as a function of temperature. The validity of the code is proved with reproducing a natural convection problem from the literature. After the validation process, time-wise and space-wise variations of local and average Nusselt numbers are investigated for different aspect ratios of the cavity, and several thermal boundary conditions. Transient temperature and velocity distributions inside the cavity with partially active vertical walls are also discussed. The Nusselt number variations that are obtained in the current work could be implemented into the transient mathematical models to evaluate the effective thermal conductivity of water, so that, reduce the computational time and also increase the accuracy.

MATERIAL AND METHOD

Definition of problem

Current work deals with the numerical investigation of transient natural convection of water in a two-dimensional cavity. Water initially remains stagnant ($u = v = 0$), and it has uniform temperature distribution ($T(x, y, 0) = T_C$). A number of early works in literature considered varying the heater and cooler positions on the vertical walls (Türkoglu and Yücel 1994; Kandaswamy *et al.*, 2007; Nithyadevi *et al.*, 2007a; Nithyadevi *et al.*, 2007b; Jmai *et al.*, 2013). It is assumed that top and bottom sides of the cavity are insulated ($dT/dy = 0$), and lateral sides are kept at constant temperature fully or partially ($\xi = H/2$). Figure 2 illustrates the case that the lateral surfaces are partially held at T_C and T_H. For all cases, the cold wall assumed to be at $T_C = 0$°C, whereas the temperature of the hot wall is varied to be $T_H = 4$, 8 and 16°C. The effect of geometry on heat transfer is also observed by changing the aspect ratio (H/W) as 0.5, 1 and 2. All parameters that have been used during this work are given in Table 1.

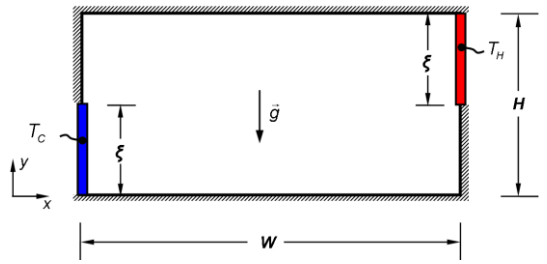

Figure 2. Mathematical model

Table 1. Numerical Parameters

Case No	ΔT	H/W	ξ
1		0.5	
2	4	1.0	H
3		2.0	
4		0.5	
5	8	1.0	H
6		2.0	
7		0.5	
8	16	1.0	H
9		2.0	
10	8	0.5	
11	8	0.5	
12	8	1.0	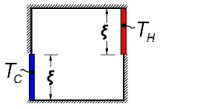
13	8	1.0	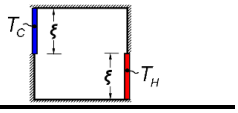

Numerical Method and Validation

For incompressible and Newtonian fluids, the time-dependent conservation equations for laminar flow are as follows;

Mass:

$$\frac{\partial}{\partial t}(\rho)+\frac{\partial}{\partial x}(\rho u)+\frac{\partial}{\partial y}(\rho v)=0 \tag{2}$$

x-momentum;

$$\frac{\partial}{\partial t}(\rho u)+\frac{\partial}{\partial x}(\rho uu)+\frac{\partial}{\partial y}(\rho vu)=-\frac{\partial p}{\partial x}+\frac{\partial}{\partial x}\left[\frac{\partial}{\partial x}(\mu u)\right]+\frac{\partial}{\partial y}\left[\frac{\partial}{\partial y}(\mu u)\right] \tag{3}$$

y-momentum;

$$\frac{\partial}{\partial t}(\rho u)+\frac{\partial}{\partial x}(\rho uv)+\frac{\partial}{\partial y}(\rho vv)=-\frac{\partial p}{\partial y}+\frac{\partial}{\partial x}\left[\frac{\partial}{\partial x}(\mu v)\right]+\frac{\partial}{\partial y}\left[\frac{\partial}{\partial y}(\mu v)\right]-g\left(\rho-\rho_{ref}\right) \tag{4}$$

Energy:

$$\frac{\partial}{\partial t}(\rho cT)+\frac{\partial}{\partial x}(\rho cuT)+\frac{\partial}{\partial y}(\rho cvT)=\frac{\partial}{\partial x}\left[\frac{\partial}{\partial x}(kT)\right]+\frac{\partial}{\partial y}\left[\frac{\partial}{\partial y}(kT)\right] \tag{5}$$

Except the specific heat of water (c), thermal conductivity (k) and viscosity (μ) are defined depending on the temperature. Thermo-physical properties of water are given in Table 2.

Table 2. Thermo-physical properties of water (Moraga and Vega, 2004)

Property	Function *or* Value
Specific Heat (J/kgK)	4204
Thermal Conductivity (W/mK)	$-0.63262+7.1959\times10^{-3}T-1.144\times10^{-5}T^2+4.2365\times10^{-9}T^3$
Density (kg/m^3)	$456.49+3.925T-0.007085T^2$
Viscosity (Ns/m^2)	$0.038208/(T-252.33)$

The numerical code is generated with control volume approach by using C++ programming language. “Power Law” scheme (Patankar, 1980) is applied to discretize the convection terms of the governing equations, and SIMPLE algorithm (Patankar, 1980) is implemented to solve the pressure-velocity coupling. Algebraic systems of discretized equations are numerically resolved by using Strongly Implicit Solver of Lee (Lee, 1990). Control volumes are stretched from the walls at a rate of 5% to capture the viscous and thermal boundary layers near the walls of the cavity. Time step-size is set as $\Delta t = 0.1$ *s* to be able to catch the time-dependent solutions, and the convergence criteria is defined for each time step as

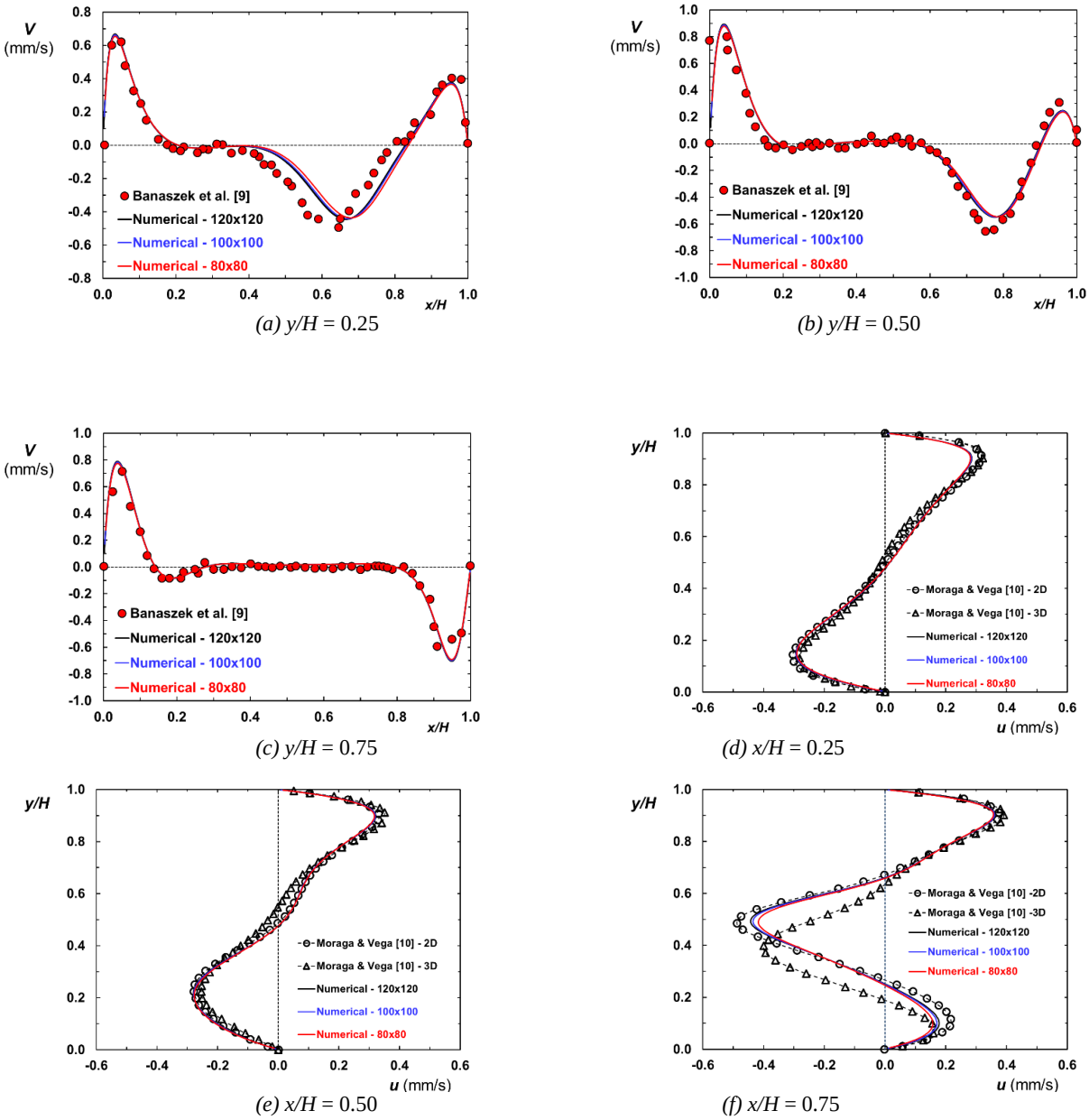

(a) y/H = 0.25 *(b) y/H* = 0.50

(c) y/H = 0.75 *(d) x/H* = 0.25

(e) x/H = 0.50 *(f) x/H* = 0.75

Figure 3. Variation of the *y*- and *x*- components of velocity with respect to position for different planes - *t* = 2400 s

$$\left|\frac{\phi^{k}-\phi^{k-1}}{\phi^{k}}\right| < 10^{-4} \qquad (6)$$

A transient natural convection problem that has been studied earlier by experimentally (Banaszek *et al.*, 1999) and numerically (Moraga and Vega, 2004) is reproduced to prove the accuracy of the current numerical code. In this problem, water is initially stagnant and at 10°C in a square cavity (*H* = *W* = 0.038 m). One side of the vertical wall is suddenly dropped to 0°C, and the buoyancy-driven convection occurs. Time-dependent flow distribution inside the cavity was obtained experimentally (Banaszek *et al.*, 1999) and numerically (Moraga and Vega, 2004). Figure 3(*a*, *b* and *c*) presents the variations of *y*- component of velocity (*v*) along the width of the cavity on several vertical positions in comparison with the reference paper (Banaszek *et al.*, 1999). In Figure 3(*d*, *e* and *f*), on the other hand, the variations of *x*-component of velocity (*u*) through the height of cavity on several horizontal positions are compared with the reference paper (Moraga and Vega, 2004). Consequently, it seems that the velocity distributions that are obtained in the current study are compatible with the experimental data that are measured by Banaszek *et al.* (1999). On the other hand, Figure 3(*d*, *e* and *f*) reveals that the current predictions have reasonable consistency with the results of the two-dimensional results of Moraga and Vega (2004). However, owing to the influence of three-dimensional flow field and side wall effects, the predicted velocity profiles at *x/H* = 0.50 and *x/H* = 0.75 differ from the results of reference paper for 3D case. The influence of the number of control volumes on the results is also examined. Comparing the predictions for 80x80, 100x100 and 120x120 of control volumes, it seems that 100x100 is an optimum choice. As a result, comparative results suggest that the current code accurately captures the transient natural convection of water in a cavity.

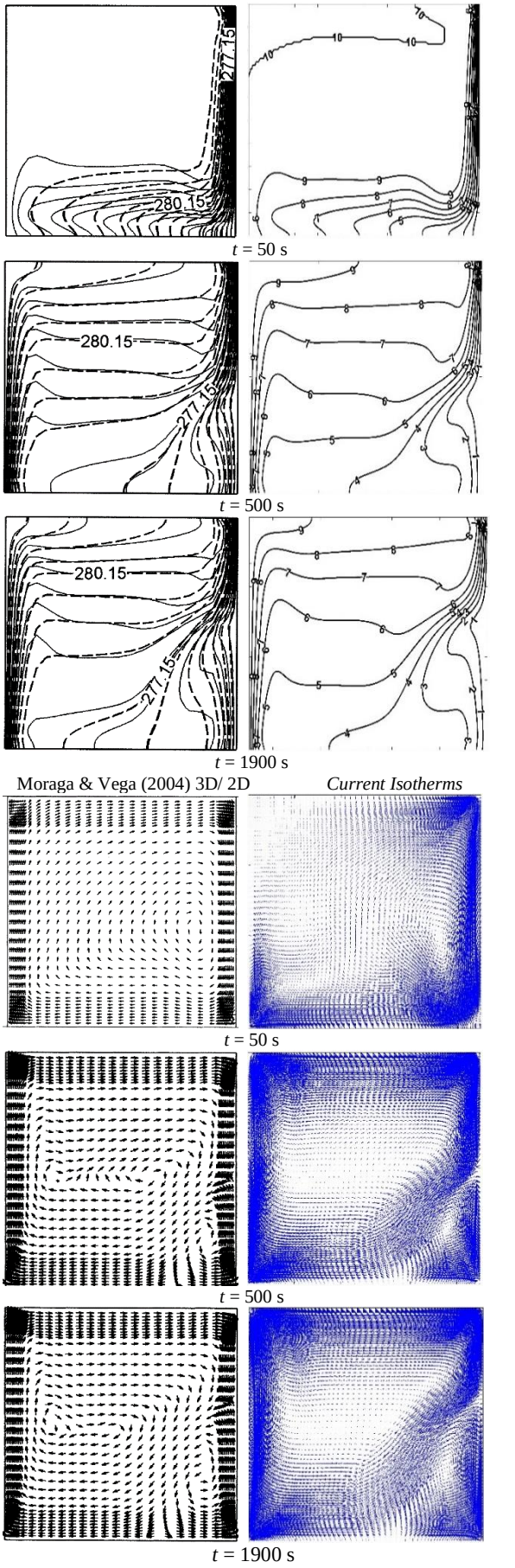

Figure 4 Transient temperature and velocity distributions inside the cavity

Figure 4 shows the isotherms and velocity vectors that are obtained at t = 50 s, 500 s and 1900 s in comparison with the numerical results that are given by Moraga and Vega (2004). Temperature distributions evaluated by our numerical code are similar to the outcome of the reference paper for 2D case. Also, comparison of current velocity vectors and the ones on the reference work show that the size of the secondary circulation cell on the cold wall coincides for t = 500 s and 1900 s.

RESULTS AND DISCUSSION

In this section, time-wise Nusselt number variations based on the geometrical and thermal parameters are given at first. After that time-dependent velocity and temperature distributions are discussed, and local Nusselt variations along the hot wall are obtained.

Average Nusselt Number

Variation of heat transfer rate can be identified in terms of the dimensionless Nusselt number. Local Nusselt number over the cold (X =0) or hot (X=1) wall is defined by using dimensionless parameters as,

$$\mathrm{Nu} = \left| \frac{\partial \theta}{\partial X} \right|_{X=0,1} \tag{7}$$

where, θ [$=\left(T - T_C\right)/\left(T_H - T_C\right)$] is the dimensionless temperature and X [=x/H] represents the dimensionless position. In order to obtain the "*area-weighted average Nusselt number*" on a surface, following definition is used,

$$\overline{\mathrm{Nu}} = \frac{1}{A}\int_0^A \left| \frac{\partial \theta}{\partial X} \right|_{X=0,1} dY \tag{8}$$

where, Y [= y/H] corresponds to the dimensionless vertical position.

Figure 5(a) shows the time-wise variation of the average Nusselt number on the cold wall. For R = 1.0 (Case #1, #2 and #3), Nusselt number exponentially increases independently from the aspect ratio. It seems that Nusselt numbers do not significantly change after t = 1500 s, which means that the problems approach the steady-state. On the other hand, for R = 0.5 (Case #4, #5 and #6), step-like changes are observed in the time-wise variations of Nusselt numbers. After a certain flow-time, a secondary circulation cell forms on the hot wall, and that may cause those alterations. For all three cases, it takes 4500 s to let the liquid reaches a steady-state condition. For R = 0.25 (Case #7, #8 and #9) sudden increments are obtained on the time-wise variation of Nusselt number after t = 300 s. Since the temperature difference is higher, secondary circulation cells forms on the hot wall in the early stages and grows up through the cold wall rapidly. It seems that that it takes 2500 s to reach a steady-state condition. For partially active heating/cooling walls, (Case #10 to #13), it is clear that the aspect ratio slightly affects the Nusselt number. For Case #11 and #13, in which the heating part is placed on the upper half of the wall, a significant difference between the Nusselt numbers is observed at the initial periods. Nusselt numbers

approach to each other with increasing time and becomes identical when the flow is reached a steady-state condition. For Case #10 and #12, the heating part is placed in the lower half of the wall. It seems that there is no significant difference between the surface Nusselt numbers. Figure 5(b) shows the variation of the average Nusselt number as a function of density inversion parameter (R) and aspect ratio (H/W) at the steady-state condition. For R = 0.25, the temperature difference between side walls are maximum (T_h = 16°C), so the Nusselt numbers have also higher values. For R = 0.5, although the hot wall temperature is T_h = 8°C, the Nusselt number is lower than the one that is obtained for R = 1.0 (T_h = 4°C). Basically, for R = 0.5, two separate circulation cells occur inside the cavity, and the increasing friction loss inversely affects the convective heat transfer.

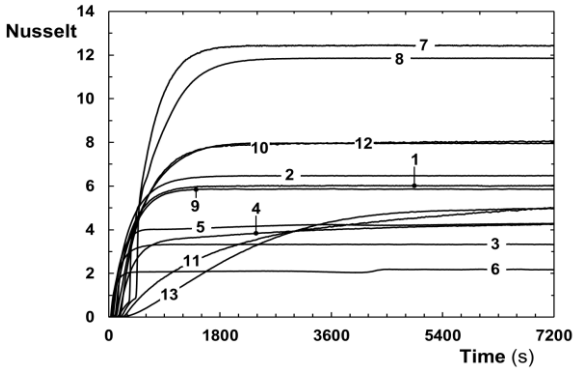

(a) *Time-wise variation*

(b) *Steady-State*

Figure 5. Nusselt number variations

Velocity and Temperature Fields

In Figure 6, isotherms and streamlines are given for the aspect ratio of (H/W) = 1.0 and R = 0.5. At t = 300 s, a secondary circulation cell appears near the bottom side of the hot wall. There are two circulation zones in the cavity that are separated by the density inversion temperature of water (T_m = 4°C). For $T > T_m$, density decreases with increasing the temperature, so that, there is a counter-clockwise circulation zone near the hot wall. On the other hand, a clockwise circulation cell is dominant for the region that is below the T_m. At t = 900 s, the secondary circulation cell grows in the vertical direction and covers the hot wall. t = 7200 s, on the other hand, represents the steady-state condition. According to the previous findings in literature (Lin and Nansteel, 1987; Wei and Koster, 1994), for the case of R = 0.5, under the steady-state condition and with constant thermo-physical properties, the density inversion temperature (T_m) divides the cavity by two equal parts. Current predictions, on the other hand, reveals that the circulation cell on the right-hand side of the cavity is bigger than the cold one, and the symmetry of the isotherms (or *streamlines*) deteriorate. Unlike from the common approach in literature (Lin and Nansteel, 1987; Wei and Koster, 1994), this study takes into account temperature dependent viscosity and thermal conductivity of water. It is well-known fact that the viscosity of water decreases with increasing the temperature. So that, the circulation cell on the right-hand side of the cavity may grow more easily owing to the lower viscosity values. For R = 0.5, the effect of friction reduces the buoyancy forces on the density inversion plane, thus the rate of heat transfer also decreases. Even though the temperature difference of R = 0.5 (ΔT = 8°C) is bigger than R = 1.0 (ΔT = 4°C), friction losses decrease the heat transfer rate or the surface Nusselt number.

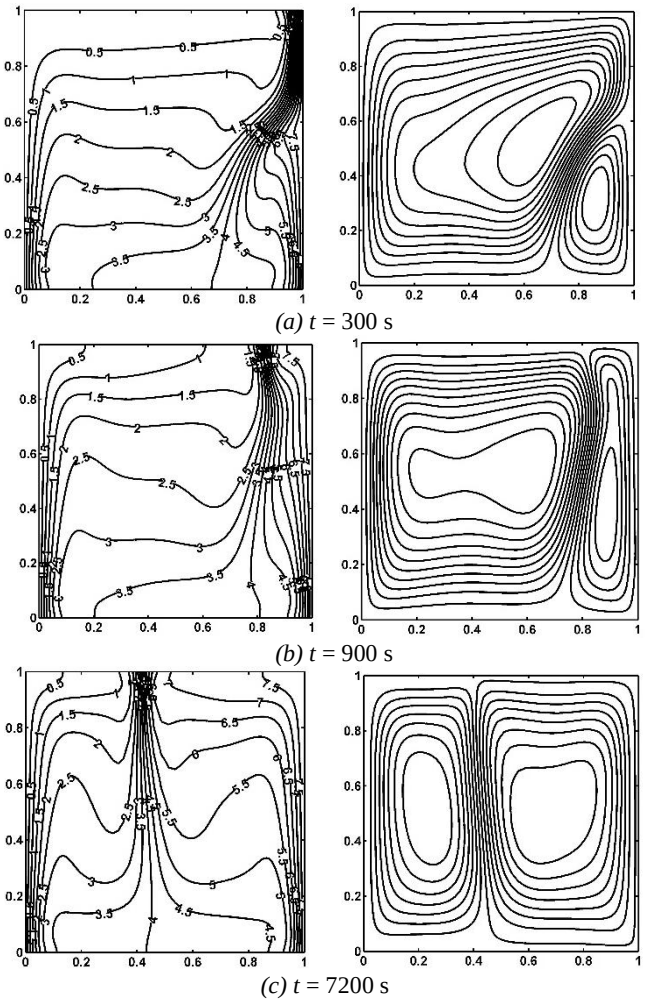

(a) t = 300 s

(b) t = 900 s

(c) t = 7200 s

Figure 6. Isotherms (*left*) and streamlines (*right*) for Case #5 (H/W) = 1.0, R = 0.5

Figure 7 shows the isotherms and streamlines at t = 300 s, 900 s and 7200 s for (H/W) = 2.0 and R = 0.5. Since the cavity height is taller than the one in Case #5, the buoyancy forces become more efficient in this geometry. At t = 300 s, the secondary circulation cell almost covers the hot wall and influential over the half of the cavity width. In the advancing time, counter-clockwise circulation cell grows through the cold wall and suppresses the clock-wise cell at

the steady-state condition. Results reveal in the tall cavities that, unlike the square case, there is no symmetry between circulation cells for $R = 0.5$.

Figure 8 indicates the natural convection characteristics in a cavity with an aspect ratio of $(H/W) = 0.5$ and $R = 0.5$. In the current geometry, the generation of secondary circulation cell near the hot wall resembles the one in the square cavity (Case #5). At $t = 300$ s, counter-clockwise circulation cell appears at the bottom side of the hot wall and grows along the vertical direction on the later on. At the steady-state condition, there are two asymmetric circulation cells and the counter-clockwise circulation cell shifts the other one to the cold wall and dominates almost 60% of the cavity width.

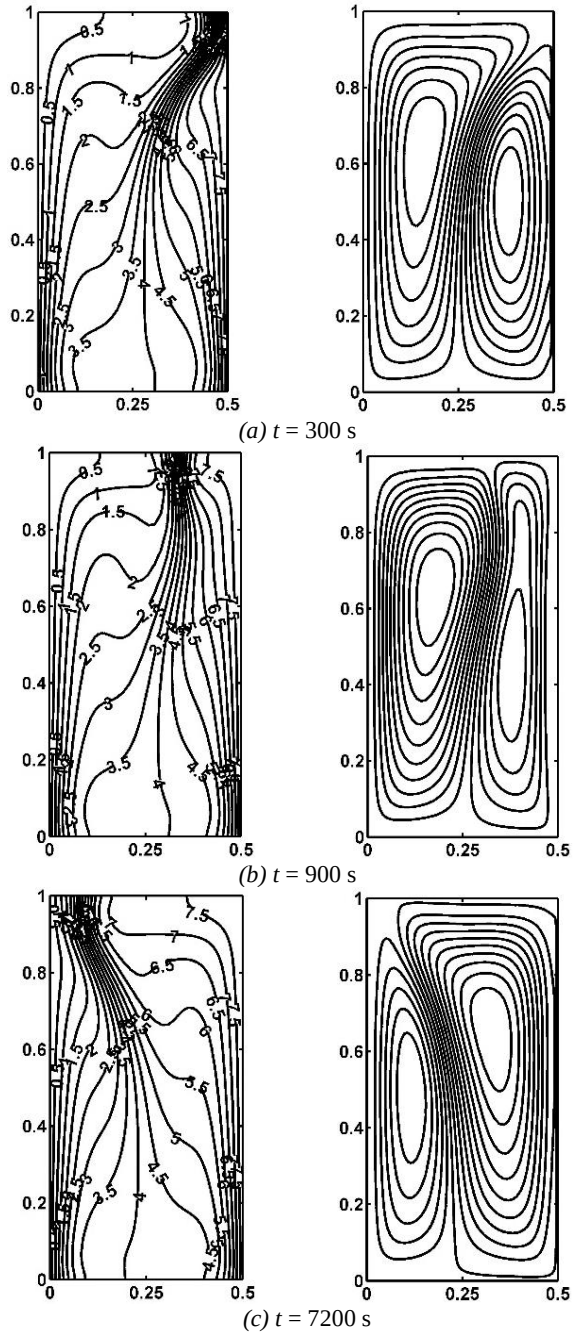

(a) $t = 300$ s

(b) $t = 900$ s

(c) $t = 7200$ s

Figure 7. Isotherms (*left*) and streamlines (*right*) for Case #6 $(H/W) = 2.0$, $R = 0.5$

In the remaining part of the paper, short ($H/W = 0.5$) and square ($H/W = 1.0$) cavities are reconsidered with partially active walls. As given in Table 1, partially active hot and cold walls are simulated for each geometry. Figure 9 represents the generation of natural convection for Case #10. While the upper half of the right wall is hot, the lower half of the left wall is cold. In comparison with the full active wall cases, the formation of secondary circulation zone is delayed. A small counter-clockwise cell is observed at $t = 900$ s on the top-right corner of the cavity. The cell grows diagonally and at the steady-state condition, it can only be effective near a small place close to the active hot-wall.

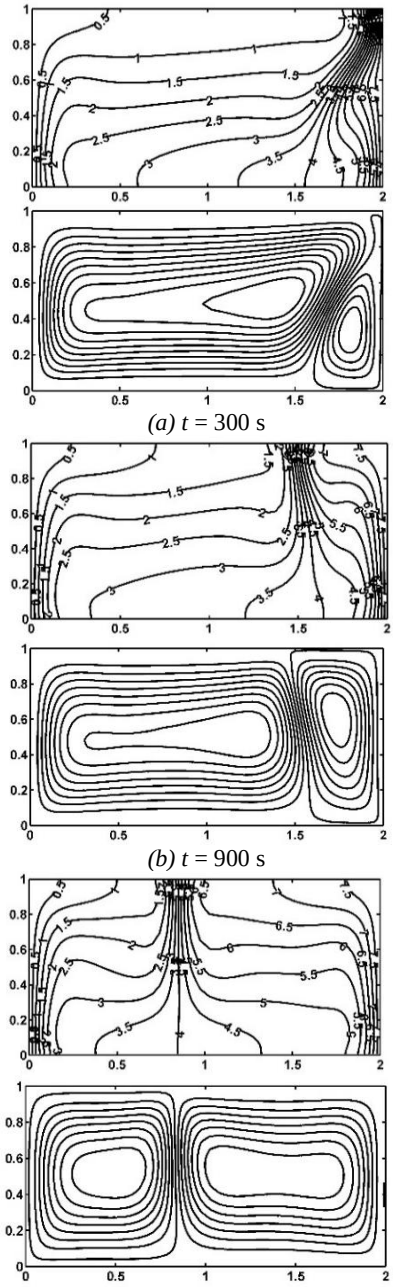

(a) $t = 300$ s

(b) $t = 900$ s

(c) $t = 7200$ s

Figure 8. Isotherms and streamlines for Case #4, $(H/W) = 0.5$, $R = 0.5$

Figure 10 gives the variation of the local Nusselt number at different flow-times. The arrow that seems in the Figure represents the increasing time. At the beginning of the process, the temperature gradients on the hot wall are higher, so that Nusselt number has maximum values at initial times. In ascending time, temperature gradients decrease at the top of the cavity so that local Nusselt number is also reduced. Since the temperature gradients are higher at the leading edge of the hot wall after t = 900 s, the sudden increment on the Nusselt number along the vertical direction becomes more remarkable in Figure 10.

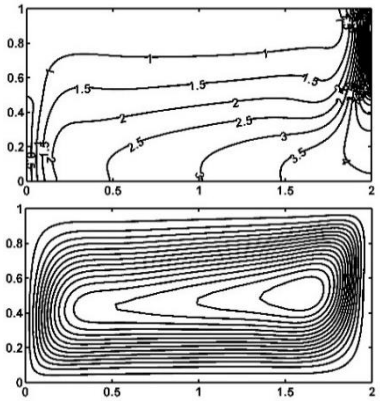

(a) t = 300 s

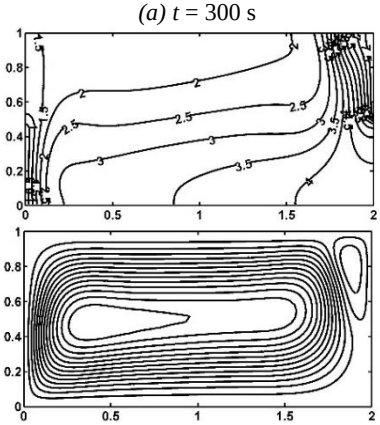

(b) t = 900 s

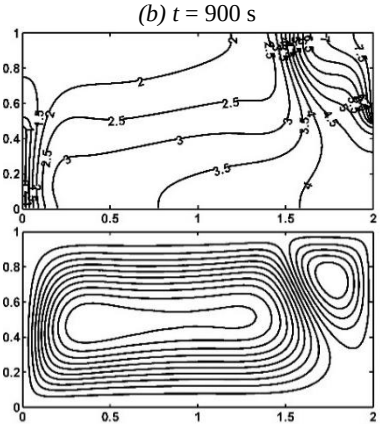

(c) t = 7200 s

Figure 9. Isotherms (*left*) and streamlines (*right*) for Case #10, (*H/W*) = 0.5, R = 0.5

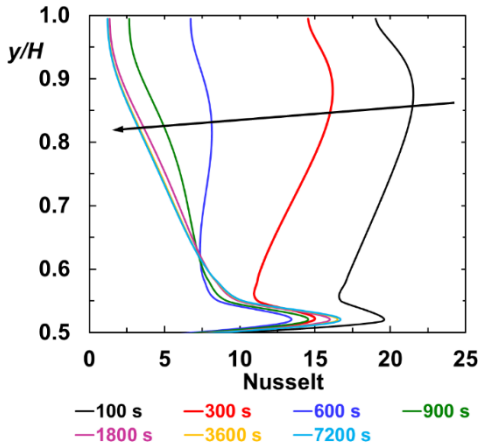

Figure 10. Time-wise variation of local Nusselt number on hot wall – *Case* #10, (*H/W*) = 0.5, R = 0.5

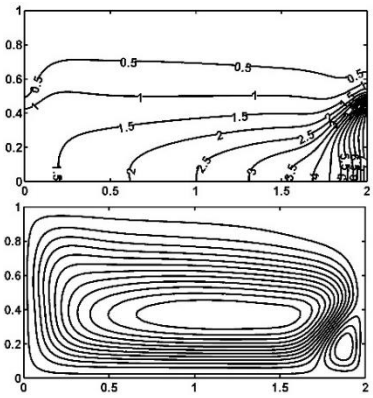

(a) t = 300 s

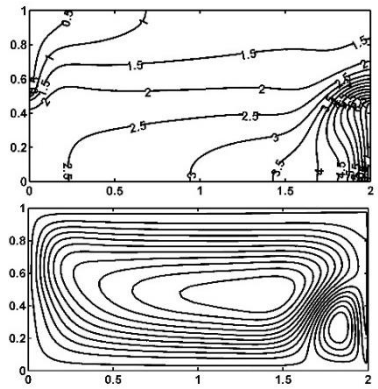

(b) t = 900 s

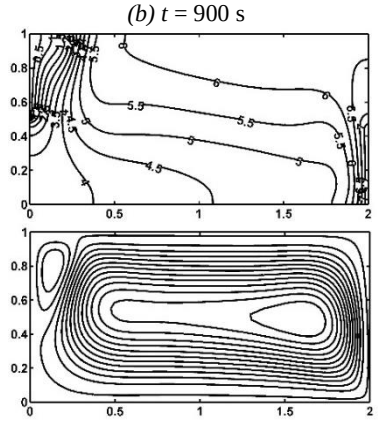

(c) t = 7200 s

Figure 11. Isotherms (*left*) and streamlines (*right*) for Case #11, (*H/W*) = 0.5, R = 0.5

Figure 11 reveals the formation of natural convection for Case #11. The lower half of the right wall is hot and the upper half of the left wall is cold. The grow rate of secondary circulation cell is higher than the one in Case #10. At steady-state condition, counter-clockwise circulation cell dominates the whole domain, but the clockwise circulation cell becomes active only near the cold wall at the top-left corner of the cavity. As seen in Figure 12, because of the higher heat transfer rates on the hot wall, Nusselt number has greater values, especially at the initial periods with respect to Case #10. The thermal plume that is obtained at the initial periods (t = 300 s and 900 s) induces the higher gradients on top of the hot wall, so that the Nusselt number values become enormous.

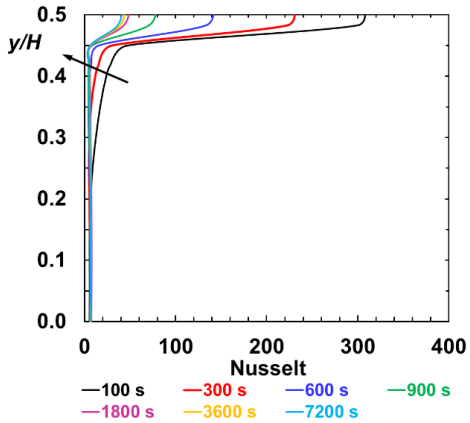

Figure 12. Time-wise variation of local Nusselt number on hot wall – *Case* #11, (*H/W*) = 0.5, *R* = 0.5

Figure 13 indicates the time-wise variation of natural convection for partially heated/cooled the square cavity for Case #12. The upper half of the right wall is hot and the lower half of the left wall is cold. Single clockwise circulation is dominant for this problem. The center of circulation cell moves from the hot wall through the middle of the cavity and extends. A weak counter-clockwise cell is observed at the steady-state condition. The variation of the local Nusselt number at selected flow times are given in Figure 14. The space-wise variations have the similar tendencies, but the magnitudes decrease in time. After t = 600 s, variations of Nusselt number are altered owing to the formation of the secondary circulation near the hot wall. Relatively higher values are also observed close to the lower half of the hot wall.

In Figure 15 and 16, isotherms, streamlines, and local Nusselt number variations are represented for Case #13. While the lower half of the right wall is hot, the upper half of the left wall is cold. Similar to the Case #11, a thermal plume is observed near the partially active hot wall at the initial periods. A secondary anti-clockwise circulation cell can be seen at t = 300 s. In time, the secondary circulation grows and dominates into the cavity. The steady state streamlines and isotherms look similar to the ones that are obtained in Case #12. It should be kept in mind that the circulation is the clockwise rotation for Case #12, on the other hand, the circulation is the counter-clockwise rotation for Case #13. Local Nusselt number variations also look alike with the Case #12. It is obvious that, Case #12 reaches the steady-state condition faster than Case #13.

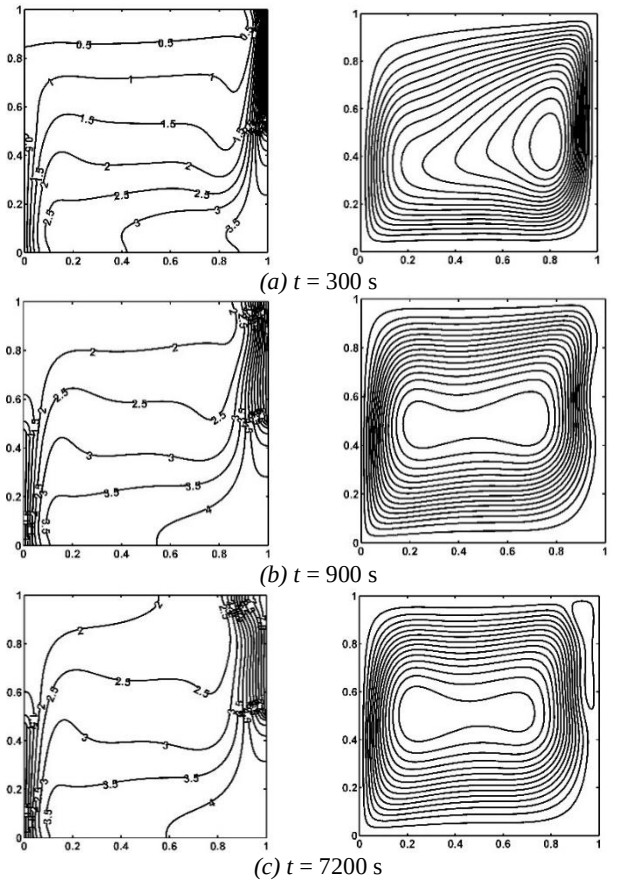

Figure 13. Isotherms (*left*) and streamlines (*right*) for Case #12, (*H/W*) = 1.0, *R* = 0.5

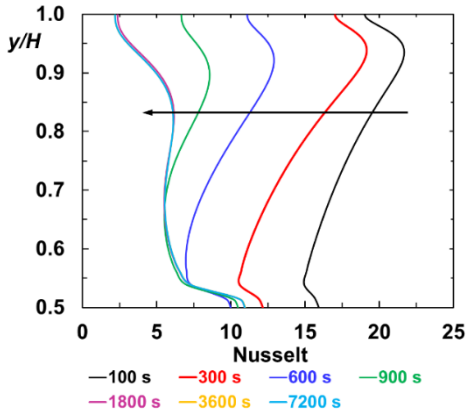

Figure 14. Time-wise variation of local Nusselt number on hot wall – *Case* #12, (*H/W*) = 1.0, *R* = 0.5

CONCLUSIONS

This study investigates the transient natural convection of water near its density inversion in a Cartesian geometry with different aspect ratios and also thermal boundary conditions. The main outcomes of the numerical analyzes are as follows,

- Considering a square cavity with side walls of T_c = 0°C and T_h = 8°C, two identical circulation cells, with opposite directions, are reported in the literature. In the current model thermo-physical properties of water (i.e. density, viscosity and thermal conductivity) are defined as a function of temperature. So the transient

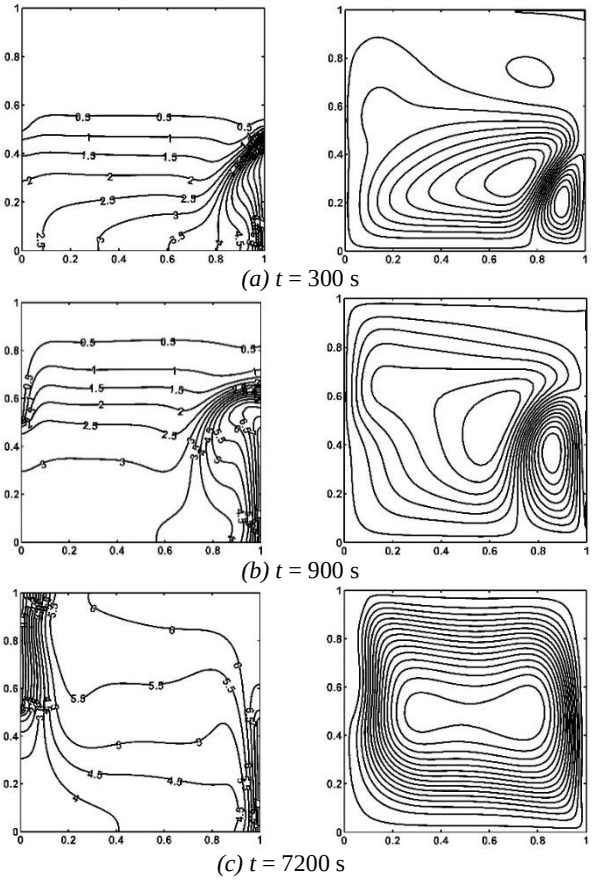

(a) t = 300 s

(b) t = 900 s

(c) t = 7200 s

Figure 15. Isotherms (*left*) and streamlines (*right*) for Case #13, (*H/W)* = 1.0, *R* = 0.5

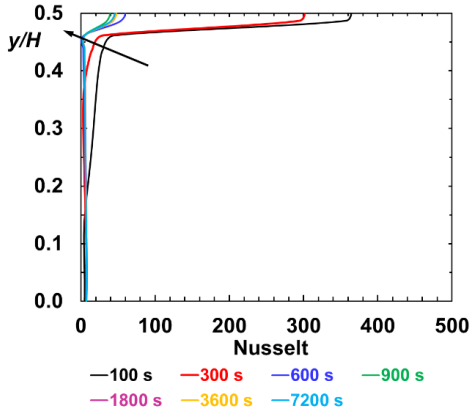

Figure 16. Time-wise variation of local Nusselt number on hot wall – *Case #*13, (*H/W)* = 1.0, *R* = 0.5

heat transfer near the cold and hot wall do not proceed symmetrically. As a result, unlike the literature, asymmetric circulation cells are observed for *R* = 0.5.

- For *H/W*> 1 the counter-clockwise circulation cell dominates the domain. On the other hand, for *H/W*<1, the flow field approaches to the symmetry, however, the counter-clockwise circulation cell shifts the density inversion line from the mid-line through the cold wall.

- For partial cooling/heating conditions, similar behaviors are observed disregarding the aspect ratio of the cavity. It is clear that heating from the upper half of the wall is not an efficient way. Secondary circulation cell could not grow through the cold wall. This can only be effective in a small area close to the hot wall. In contrast, heating from the lower part of the wall enhances the heat transfer. The counter-clockwise circulation grows rapidly and become dominant for the entire domain at the steady state condition.

REFERENCES

Banaszek J., Jaluria Y., Kowalewski T. A. and Rebow M., 1999, Semi-Implicit FEM Analysis of Natural Convection in Freezing Water, *Numerical Heat Transfer: Part A: Applications*, 36, 449−472.

Bergman T. L., Incropera F. P. and Lavine A. S., 2011, *Fundamentals of Heat and Mass Transfer* (Seventh Ed.), John Wiley & Sons.

Braga S. L. and Viskanta R., 1992, Transient Natural Convection of Water Near its Density Extremum in a Rectangular Cavity, *International Journal of Heat and Mass Transfer*, 35, 861−875.

Ezan M. A., Uzun M. and Erek A., 2014, A Study on Evaluation of Effective Thermal Conductivity for Spherical Capsules, *The 10th International Conference on Heat Transfer, Fluid Mechanics and Thermodynamics*, Florida, 427−433.

Heier J., Bales C. and Martin V. 2015, Combining Thermal Energy Storage with Buildings–a Review, *Renewable and Sustainable Energy Reviews*, 42, 1305−1325.

Hossain M. A. and Rees D. S., 2005, Natural Convection Flow of Water Near its Density Maximum in a Rectangular Enclosure Having Isothermal Walls with Heat Generation, *Heat And Mass Transfer*, 41, 367−374.

Inaba H. and Fukuda, T., 1984, Natural Convection in an Inclined Square Cavity in Regions of Density Inversion of Water, *Journal of Fluid Mechanics*, 142, 363−381.

Ismail K. A., Henriquez J. R., and Da Silva T. M., 2003, A Parametric Study on Ice Formation Inside a Spherical Capsule, *International Journal of Thermal Sciences*, 42, 881−887.

Jmai R., Ben-Beya B. and Lili T., 2013, Heat Transfer and Fluid Flow of Nanofluid-Filled Enclosure with Two Partially Heated Side Walls and Different Nanoparticles, *Superlattices and Microstructures*, 53, 130−154.

Kandaswamy P., Sivasankaran S. and Nithyadevi N., 2007, Buoyancy−Driven Convection of Water Near Its Density Maximum with Partially Active Vertical Walls, *International Journal of Heat and Mass Transfer*, 50, 942−948.

Lee S. L., 1990, A Strongly Implicit Solver for Two-dimensional Elliptic Differential Equations, *Numerical Heat Transfer, Part B Fundamentals*, 16, 161−178.

Li G., Hwang Y. and Radermacher R., 2012, Review of Cold Storage Materials for Air Conditioning Application, *International Journal of Refrigeration*, 35(8), 2053−2077.

Lin D. S. and Nansteel M. W., 1987, Natural Convection Heat Transfer in a Square Enclosure Containing Water Near its Density Maximum, *International Journal of Heat and Mass Transfer*, 30, 2319−2329.

Mahapatra P. S., Manna N. K. and Ghosh K., 2015, Effect of Active Wall Location in a Partially Heated Enclosure, *International Communications in Heat and Mass Transfer*, 61, 69−77.

McDonough M. W. and Faghri A., 1994, Experimental and Numerical Analyses of the Natural Convection of Water Through its Density Maximum in a Rectangular Enclosure. *International Journal of Heat and Mass Transfer*, 37, 783−801.

Moraga N. O. and Vega S. A., 2004, Unsteady Three-Dimensional Natural Convection of Water Cooled Inside a Cubic Enclosure, *Numerical Heat Transfer, Part A: Applications*, 45, 825−839.

Nardini G. and Paroncini M., 2012, Heat Transfer Experiment on Natural Convection in a Square Cavity with Discrete Sources, *Heat and Mass Transfer*, 48, 1855−1865.

Nithyadevi N., Sivasankaran S. and Kandaswamy P., 2007a, Buoyancy−Driven Convection of Water Near Its Density Maximum with Time Periodic Partially Active Vertical Walls, *Meccanica*, 42, 503−510.

Nithyadevi N., Kandaswamy P. and Lee J., 2007b, Natural Convection in a Rectangular Cavity with Partially Active Side Walls, *International Journal of Heat and Mass Transfer*, 50(23), 4688−4697.

Öğüt E. B., 2010, Eğik Kare Kapalı Bir Bölge İçindeki Su Bazlı Nanoakışkanların Doğal Taşınımla Isı Transferi, *Isi Bilimi ve Tekniği Dergisi/Journal of Thermal Science & Technology*, 30, 23−33.

Öztuna S. and Kahveci K., 2013, Natural Convection Heat Transfer of Nanofluids in a Partially Divided Enclosure, *Isı Bilimi ve Tekniği Dergisi/Journal of Thermal Science & Technology*, 33, 139−154.

Patankar S., 1980, *Numerical Heat Transfer and Fluid Flow*. CRC Press.

Rahimi M., Ranjbar A. A., Hosseini M. J. and Abdollahzadeh M., 2012, Natural Convection of Nanoparticle–water Mixture Near Its Density Inversion in a Rectangular Enclosure, *International Communications in Heat and Mass Transfer*, 39, 131−137.

Rashidi I., Mahian O., Lorenzini G., Biserni C. and Wongwises S., 2014, Natural Convection of Al_2O_3/Water Nanofluid in a Square Cavity: Effects of Heterogeneous Heating, *International Journal of Heat and Mass Transfer*, 74, 391−402.

Tekkalmaz M., 2015, Numerical Analysis of Combined Natural Convection and Radiation in a Square Enclosure Partially Heated Vertical Wall, *Isı Bilimi ve Tekniği Dergisi/Journal of Thermal Science & Technology*, 35, 99−106.

Türkoglu H. and Yücel N., 1995, Effect of Heater and Cooler Locations on Natural Convection in Square Cavities, *Numerical Heat Transfer, Part A: Applications*, 27, 351−358.

Seki N., Fukusako S. and Inaba H. 1978, Free Convective Heat Transfer with Density Inversion in a Confined Rectangular Vessel, *Wärme-und Stoffübertragung*, 11, 145−156.

Wei T. and Koster J. N., 1994, Density Inversion Effect on Transient Natural Convection in a Rectangular Enclosure, *International Journal of Heat and Mass Transfer*, 37, 927−938.

M. Akif EZAN is an Assistant Professor in the Department of Mechanical Engineering at Dokuz Eylul University. He received his Ph.D. degree from the same university in 2011. He was in UOIT, Oshawa, Canada, as a visiting researcher in 2010, for one year. He is author or co-author of more than 40 technical papers in the international journals or conferences. His main research interests are phase change materials, thermal management, and numerical heat transfer & fluid flow.

Mustafa KALFA was born in Trabzon-Turkey in 1989. He received his BSc degree in Mechanical Engineering at Cukurova University in 2012. He is currently a MSc student at Dokuz Eylül University, Department of Thermodynamics. He is also working as an R&D Engineer in a multinational company. His main interests are numerical heat transfer & fluid flow.